

# **CVD Diamond Vacuum Window for Synchrotron Radiation Beamlines**

Heinrich Blumer<sup>\*</sup>, Saša Zelenika<sup>#</sup>, Jakob Ulrich<sup>\*</sup>, Robin Betemps<sup>\*</sup>, Lothar Schulz<sup>\*</sup>, Franz Pfeiffer<sup>\*</sup>,  
Uwe Flechsig<sup>\*</sup>, Urs Ellenberger<sup>\*</sup>, Christoph Wild<sup>+</sup>

<sup>\*</sup>Paul Scherrer Institut, 5232 Villigen PSI, Switzerland

<sup>#</sup>University of Rijeka –Faculty of Engineering, Vukovarska 58, 51000 Rijeka, Croatia

<sup>+</sup>Diamond Materials GmbH, Tullastrasse 72, 79108 Freiburg, Germany

## *Abstract*

*An innovative design of a chemical vapour deposited (CVD) diamond vacuum window is presented. The thermo-mechanical properties of the integrated window have been optimised through extensive numerical modelling. An innovative brazing procedure suited for thin non-metallised windows was concurrently developed. Mechanical and optical tests performed on the prototype of the window confirmed the validity of the adopted concepts, thus providing proof that the developed solution constitutes a valid and in many aspects advantageous solution with respect to beryllium windows so far used at synchrotron radiation facilities for this purpose. Based on the proposed design, an off-the-shelf diamond window is being brought to market.*

## **1. Introduction**

At synchrotron radiation (SR) facilities around the world, beryllium (Be) windows are used as standard beamline front-end components. In fact, due to its low atomic number resulting in good optical transmission, as well as rather good thermal properties, Be has long been the material of choice for front-end windows. Be windows have generally two functions: a first thicker window absorbs the low energy photons (lowering the heat load on the downstream components), while the second, generally thin, Be window, separates the ultra high vacuum of the storage ring from the beamline environment (often this window has also the safety function of absorbing the pressure wave of an accidental downstream inrush of air) [1].

Despite these advantages, in SR applications requiring high synchrotron beam quality, Be shows also drawbacks, the main being coherence degradation due to the roughness of the Be foil (leading to phase shifts), as well as to Fresnell diffraction on the surface pits and voids of the foil [2]. For these reasons, an increased attention is being dedicated to the development of CVD (chemical vapour deposition) diamond windows. In fact, the optical quality of CVD diamond allows today the problems encountered in the usage of Be to be avoided. Moreover, CVD diamond has also excellent thermal and mechanical properties [3], which could allow both functions of the Be front-end windows to be combined in a single diamond vacuum window. The challenge with the latter solution lies in the low thermal expansion of diamond, resulting in big differential thermal expansions with respect to the window frame material. A further challenge is represented also by the brazing process of thin diamond foils to the window frame material so to achieve the desired vacuum tightness.

An optimised design of a CVD diamond vacuum window for the Swiss Light Source (SLS) beamlines is presented in this work. The single diamond window has in this case both the functionality of a thermal filter, as well as of a vacuum and safety element. Results of a numerical optimisation of the mechanical behaviour of the window in the case on an air inrush, as well as its thermal behaviour during brazing, bake-out and under photon beam absorption are given. Thermo-mechanical and optical tests performed on the prototype of a high vacuum brazed window are also presented.

## **2. Mechanical Properties of CVD Diamond Compared to Beryllium**

CVD diamond is characterised by high thermal conductivity and hardness, as well as excellent optical properties. In fact, although its atomic number  $Z$  is higher than that of Be and thus its absorption is higher, this is highly compensated by the thermal conductivity  $\lambda$  (which implies that the absorbed

energy is quickly dissipated to the edges where it can be removed by appropriate heat sinks and cooling, resulting also in reduced stresses) and strength  $\sigma$  (which makes possible the usage of thinner foils) of CVD – Table 1. Taking then into account the thermal figure of merit which is proportional to  $\lambda/Z^2$  and the structural figure of merit which is proportional to  $\lambda/(Z^2 \cdot E \alpha)$  [4], CVD diamond is 4 and 17 times respectively more advantageous than Be. Moreover, contrary to Be which can be hardly machined due to the toxicity of its pulverised particles, CVD can be produced with a homogeneous thickness (which is often not the case with Be), laser cut to various shapes and polished down to nanometric levels [5]. A significantly smaller degradation of the quality of synchrotron beams has thus been shown in several applications [6-8]. In these applications, however, the CVD window was executed in a configuration which was either not vacuum tight (i.e. it was just used as a thermal filter) or it was joined with a low thermal expansion material, which thus leads to the degradation of heat conductivity to the heat sink.

*Table 1: Comparison of mechanical properties of CVD diamond and beryllium*

Property	CVD diamond	Beryllium
Atomic number $Z$	6	4
Hardness (kg/mm <sup>2</sup> )	12000 – 15000	150 – 200
Tensile strength $\sigma_{tens}$ (MPa)	> 1200	80 – 550
Density $\rho$ (g/cm <sup>3</sup> )	3.52	1.85
Young's modulus $E$ (GPa)	1140	290
Poisson's ratio $\nu$	0.069	0.02 – 0.08
Specific heat $c$ (J/(gK))	0.52	1.87
Thermal expansion coefficient $\alpha$ ( $\mu\text{m}/(\text{mK})$ )	1.1 (at RT) 2.6 (20 – 500°C)	11.6 (at RT) 15.0 (25 – 500°C)
Thermal conductivity $\lambda$ (W/(mK))	2000 (at RT) 730 (at 500°C)	180 (at RT) 97 (at 540°C)
Optical transparency	UV to far IR	Opaque
Resistivity ( $\Omega\text{cm}$ )	Insulator: $10^{13} - 10^{16}$	Conductor $4.1 \cdot 10^{-6}$
Melting temperature	at 1500°C diamond transforms to graphite	1285°C
Toxicity	None	High (even small amounts can cause severe health hazards)

### 3. Numerical Optimisation of the Mechanical Design

The design was optimised for the bending magnet beamlines working at energies neighbouring the SLS critical photon energy (5.35 keV). Given the necessary beam acceptance (the window was to be mounted at 5.5 m from the source within the machine shielding wall and accept  $0.4 \times 3$  mrad), as well as the necessary flux (a transmissibility of at least 50% at the considered energy was required) for the foreseen applications, the chosen window had to have an elliptical shape of  $6 \times 18$  mm with a thickness of 100 – 250  $\mu\text{m}$  (depending on the beamline being considered).

A thorough thermal and mechanical analysis was performed on an integrated window of such shape using the finite element method (FEM). Due to the thermal requirements of absorbing and dissipating up to 160 W of beam energy, oxygen free high conductivity copper (OFHC Cu) with a suitable cooling system (keeping the edge of the Cu block at 30°C) was adopted as the window frame material. Solid elements were then used to model numerically this frame, while shell elements were used for modelling the CVD foil itself.

#### 3.1. Optimisation of the Thermal Behaviour

As it was already pointed out, an innovative brazing procedure was developed in the frame of the proposed solution. In fact, an active high vacuum brazing process not necessitating the metallisation of the window foil was pursued. This has advantages in terms of the optical performances, in terms of the production times and costs, as well as in the fact that the resulting window can then be baked-out to high temperatures ( $\geq 250^\circ\text{C}$ ). A suitable brazing alloy which allows the formation of the active layer at

the CVD-to-Cu interface and that allows the best wetting of this interface [9] was thus chosen. Given, however, the high solidus temperature of the alloy (ca. 750°C), a suitable design had to be found. This is based on a compliant region which can accommodate the differential thermal expansion effects (CVD has the above listed expansion coefficient  $\alpha$ , while that of Cu is 18  $\mu\text{m}/(\text{m}\cdot\text{K})$ , i.e. more than 6 times higher), while concurrently taking into account also the possible occurrence of a bi-metallic type effect (with the resulting bending stresses in the CVD foil) which could lead to the loss of the structural integrity of CVD. The structure resulting from an iterative optimisation process (Fig. 1) allows not only to take into account all these effects, but also to keep at acceptable levels the stresses in the operative conditions with a beam power thermal absorption of 160 W. In the latter case the temperature on the foil reaches a maximum of ca. 330°C in the centre of the foil and decreases to 230°C on the transition to the copper block (Fig. 2). Given the chosen brazing procedure and alloy, this temperature levels are acceptable, as are the resulting stresses of 377 MPa in the centre of the diamond foil.

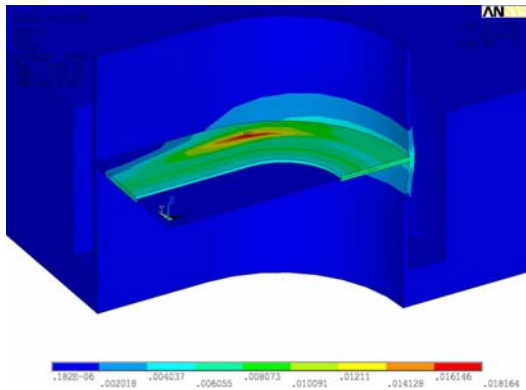


*Fig. 1: Stress distribution on the window during cooling from the brazing process. The Cu edge experiences some plastic deformation, but given its mechanical properties after brazing (high ductility) this does not imply any practical problems*

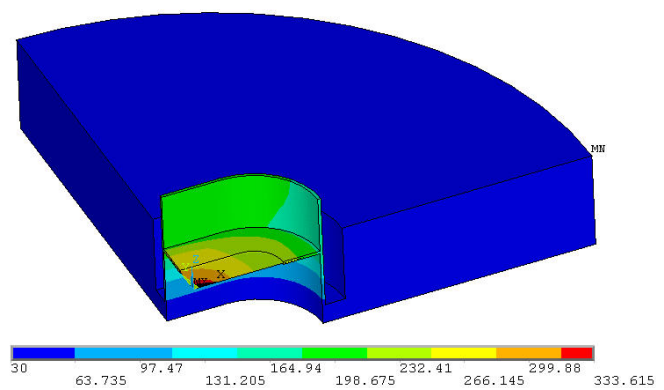


*Fig. 2: Temperature distribution in °C resulting from a heat load of 160 W applied in the centre of the window (beam footprint: 6 x 3.3 mm, window thickness: 200  $\mu\text{m}$ )*

Eventual problems could occur only if a miss-steered beam would impinge exactly on the brazing location which would imply its heating already after 0.1 – 0.2 seconds to temperatures that could endanger the integrity of the window. For this reason on the upstream side of the window assembly a suitable OFHC Cu aperture has been added to the design (Fig. 3) – for obvious reasons in the final configuration this aperture was executed with a suitable taper.

### **3.2. Optimisation of the Mechanical Behaviour**

Given the safety function the foreseen window has to have, in the FEM analysis two cases of structural load were considered: a 1 bar (0.1 MPa) pressure difference on the two sides of the window (during slow aeration of the beamline), and an accidental pressure wave coming from the experimental side of the beamline on which the window is mounted (i.e. from downstream with respect to the window itself). In the first case a stress of ca. 300 MPa in the centre of the foil is generated (Fig. 4). Even when in this configuration the beam would still be impinging on the window, it could operate with a suitable safety factor. However, when a pressure wave would be speeding from downstream, an equivalent pressure of almost 5 bar would be generated on the foil (Fig. 5a) which would cause its breakage. A suitable solution here was an introduction of an 18 mm circular diaphragm 20 cm downstream of the window, which allows the dynamic effect of the pressure wave on the foil to be reduced down to a level of 1.25 bar (Fig. 5b).

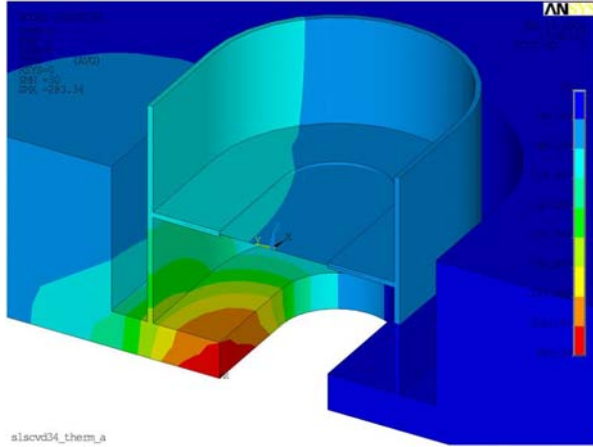


Fig. 3: Temperature ( $^{\circ}\text{C}$ ) distribution on the aperture which protects the brazing location from a miss-steered beam

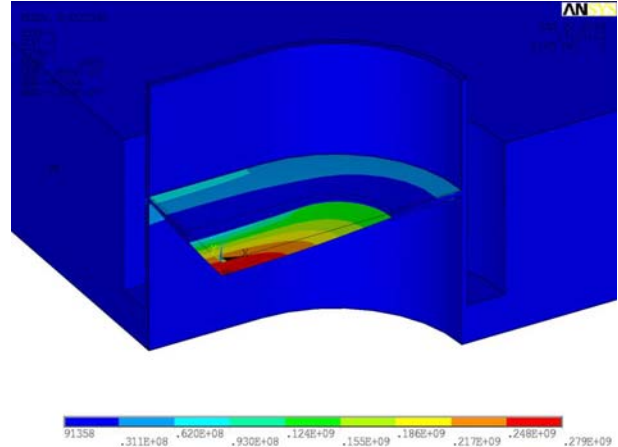


Fig. 4: Stress distribution on the CVD foil when a pressure difference of 1 bar between the two sides of the foil occurs

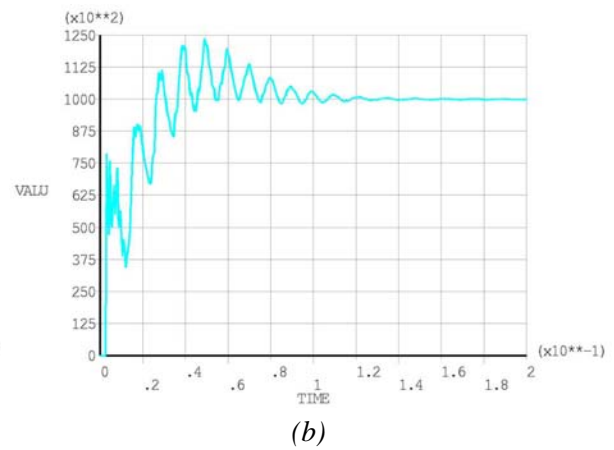
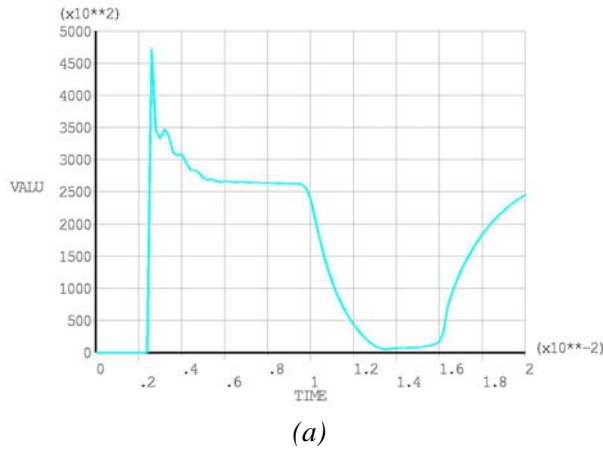


Fig. 5: Pressure wave effect (Pa) on the CVD foil without (a) and with (b) a diaphragm mounted downstream of it

## 4. Prototype Window

The designed  $100\ \mu\text{m}$  thick CVD diamond window has been integrated on a double side DN63CF flange (Fig. 6). A careful frame production and especially brazing procedure with strictly defined brazing phases for the integration of the CVD foil (Fig. 7), the Cu aperture and the cooling system was defined. On the obtained integrated structure a support for the alignment reference marks was also added. Leak rates lower than  $10^{-10}$  mbar $\cdot$ l/s have been measured on this prototype. The structure was thus considered suitable for the subsequent structural and optical tests.

## 5. Tests Performed on the Prototype Window

### 5.1. Structural Testing

The window was mounted on a vacuum system resembling as much as possible the foreseen beamline configuration (including the diaphragm). First an increasing pressure wave on the downstream side of the window was generated and, as expected, up to a 2 bar pressure wave no negative effects on the window occurred.

A static pressure was then applied to the window, which was finally broken only at an absolute pressure of 4.3 bar.

The irradiation of the window with the beam producing a heat load of ca. 100 W on the foil was also performed and no detrimental effects could be observed.

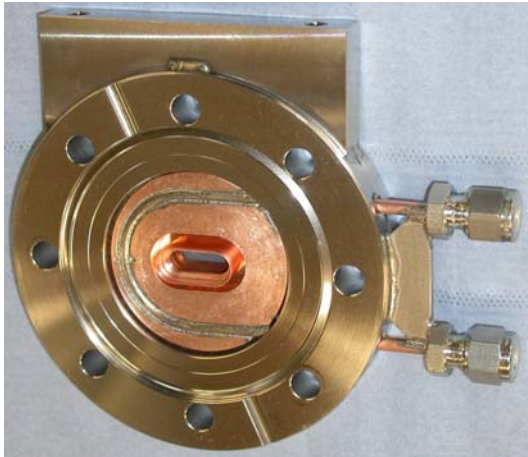


Fig. 6: Integrated DN63CF CVD diamond vacuum window with the water cooling and alignment systems



Fig. 7: Detail of the brazing of the CVD foil to the OFHC Cu frame

## 5.2. Optical Measurements

### 5.2.1. Surface Roughness Measurements

The surface roughness of the 100  $\mu\text{m}$  thick CVD diamond foil on the prototype window was measured by employing the Zygo NewView 5010 white light interferometer characterised by a roughness measurement resolution better than 0.1 nm. A three dimensional plot of the surface roughness with a peak to valley (p-v) value of 16 nm and with a root-mean-square (rms) surface roughness of 2.4 nm has been measured (Fig. 8). During a similar measurement performed on a high quality (PF60) Be window with a thickness of 75  $\mu\text{m}$ , a p-v value of 7  $\mu\text{m}$  with a 630 nm rms roughness was obtained. The CVD diamond shows thus not only a much better surface smoothness, but also a much smaller variation of the foil thickness.

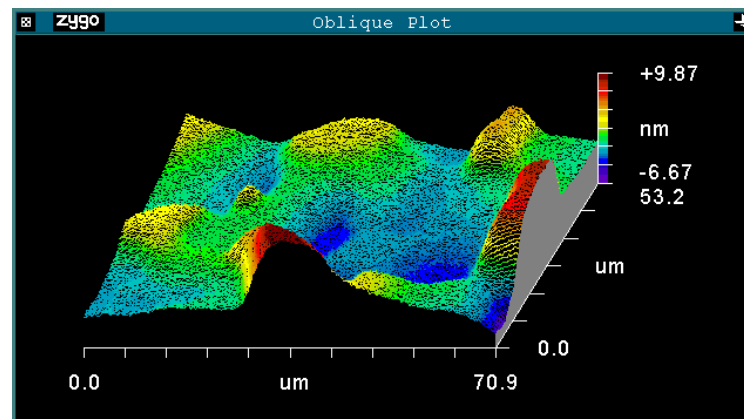


Fig. 8: Roughness measurement on the brazed CVD diamond foil: p-v roughness: 16 nm; rms roughness: 2.4 nm

### 5.2.2. Transmissibility Measurements

The transmissibility of the brazed and a “raw” (as produced) CVD diamond foil was measured at the SLS materials science beamline. The respective setup is shown in Fig. 9a. Two gas cells have been used to measure the beam intensity upstream and downstream of the window. The collimated beam size was limited to 2 x 1 mm with a slit system directly upstream of the first gas cell. An integration time of 10 seconds with the highest sensitivity of the counter cards was used. In cases when the intensity was too high (the counters went into saturation) the attenuators (absorption foils) of the beamline have been applied. No difference between the brazed and the raw window could be measured (Fig. 9b). What is

more, the measurements agree very well with the theoretical prediction for a 100  $\mu\text{m}$  diamond foil. No measurable contamination of the surface of the foil due to brazing alloy elements could be detected either.

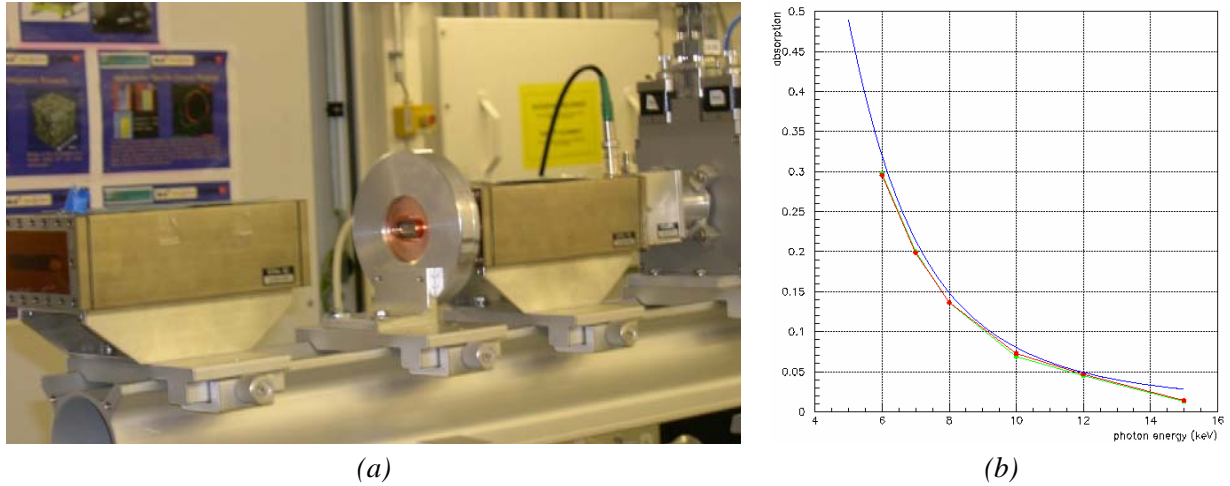


Fig. 9: Measurement set-up for the CVD diamond foil transmissibility measurements (a) and results obtained on the brazed (red line) and raw (blue line) foil (b)

### 5.2.3. Influence of the CVD Diamond Window on the Coherence of Synchrotron Radiation

Coherence properties of X-ray beams (and of any phase-shifting devices along the beamline) may be characterized by using a shearing interferometer technique and by observing a magnified Moiré-type fringe pattern on a large pixel-sized standard X-ray detector [10]. The arrangement of the thus used transmission-type interferometer consists of a beam splitting phase grating and of a slightly tilted analyzer grating which provides the spatial resolution required on a standard X-ray detector. Parts of the X-ray beams of the same source interfere in the detector plane and show a “magnified” (Moiré-effect) fringe pattern caused by a small or “shear” tilt angle (on the order of  $0.5^\circ$ ) between the gratings. From the observed fringe pattern, the resulting normalized intensity distribution  $|\gamma|$  can be calculated.

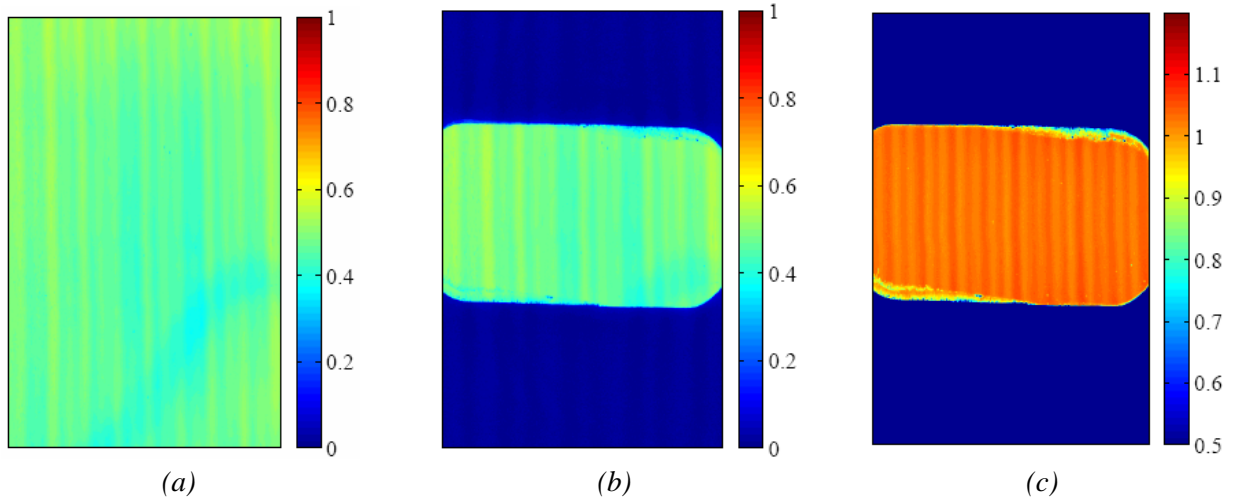


Fig. 10: Normalized intensity distribution  $|\gamma_1|$  of the beam without the CVD diamond window (a), normalised intensity distribution  $|\gamma_2|$  with the inserted window (b) and ratio of the intensity distributions  $|\gamma_2|/|\gamma_1|$  (c)

The experiment aimed at characterising the respective performances of the here developed CVD diamond vacuum window was performed at the European Synchrotron Radiation Facility (ESRF) in Grenoble, France, with 17.5 keV X-rays. The obtained fringe pattern shows the coherence of the X-ray beam (plus any phase-shifting elements along the beamline) without (normalized intensity distribution

$|\gamma_1|$  in fig. 10a) and with the inserted CVD diamond window (normalized intensity distribution  $|\gamma_2|$  of Fig. 10b). The ratio of intensity distributions  $|\gamma_2|/|\gamma_1|$  is shown in Fig. 10c. The fringe pattern of the X-ray beam affected only by the CVD diamond foil remains unaltered, i.e. it is demonstrated that the CVD diamond window does not influence significantly X-ray beam coherence.

## 6. Conclusions

The herein proposed innovative mechanical design of a CVD diamond vacuum window allows to combine both the thermal filtering and the vacuum and pressure safety functions of the so far used pair of Be windows in a single thin diamond window with excellent thermo-mechanical and optical properties. Moreover, the developed brazing procedure makes unnecessary the metallisation of the foil material, which also has advantages in terms of the optical quality of the window. In fact, the developed solution was shown to have virtually no influence on X-ray beam coherence. The adoption of high vacuum brazing makes the window also bakeable at high temperatures, and thus the UHV conditions easier to reach.

After completion of the thorough thermo-mechanical and optical tests on the prototype windows, a production of ready-to-use vacuum windows has been initiated, and the windows have been successfully installed on the SLS X02DA Tomcat and X05DA Optics beamlines. Further employment of the design is planned for several new SLS bending magnet beamlines, while concurrently variants of the described designs are being developed for different heat load levels (well below 100 W and well above 160 W) and for different X-ray beam sizes.

Based on the presented window design, an off-the-shelf CVD diamond window solution is also being brought to market through Diamond Materials GmbH [3].

## 7. Acknowledgments

The authors acknowledge the support of the technical staff of PSI. We acknowledge especially the contribution of R. Schraner and M. Kleeb in the production of the CVD diamond vacuum windows, and of X. Wang in some of the numerical calculations.

## 8. References

- [1] A. Gambitta et al., “Beryllium windows for the X-ray diffraction beamline at Elettra”, Sincrotrone Trieste Internal Publication No. ST/S-TN-93/59, 1993.
- [2] S. Goto et al., “Characterisation of Beryllium Windows Using Coherent X-rays at 1-km Beamline”, Proceedings of the 8<sup>th</sup> International Conference on Synchrotron Radiation Instrumentation, San Francisco (CA, USA) 2003, pp. 400-403.
- [3] <http://www.diamond-materials.com/>
- [4] A. M. Khounsary, “Thermal, structural, and fabrication aspects of diamond windows for high power synchrotron x-ray beamlines”, Proceedings SPIE Vol. 1739 – High Heat Flux Engineering (1992) 266-281.
- [5] Fraunhofer Institute for Applied Solid-State Physics data
- [6] J.-C. Biasci, B. Plan, L. Zhang, “Design and Performance of ESRF high-power undulator front-end components”, Journal of Synchrotron Radiation 9 (2002) 44-46.
- [7] J. V. Flaherty, Private Communication.
- [8] U. Schade, Private Communication.
- [9] A. Palavra et al., “Wettability studies of reactive brazing alloys on CVD diamond plates”, Diamond and Related Materials 10 (2001) 775-780.
- [10] F. Pfeiffer et al., “Shearing interferometer for quantifying the coherence of hard x-ray beams” Physical review letters PRL 94, 164801 (2005)